RSC Advances

ROYAL SOCIETY OF CHEMISTRY

www.rsc.org/advances

Electrochemical degradation of perfluorooctanoic acid (PFOA) by Yb-doped Ti/SnO_2-Sb/PbO_2 anodes and determination of the optimal conditions.

Qianchi Ma[a], Lei Liu[a], Wei Cui[a], Ruifeng Li[a], Tingting Song[b], Zhaojie Cui[a,*]

a, School of Environmental Science and Engineering, Shandong University, 27 Shandananlu, Jinan, 250100, China

b, Shandong Province Guohe Circular Econmy Research Center

Corresponding author. Tel:+(86)0531-88361176; fax: + (86)0531-88361176

E-mail address: cuizj@sdu.edu.cn

ABSTRACT

Model aqueous solutions of perfluorooctanoic acid (PFOA, 100 mg/L) were electro-oxidized in a homemade container. The electrocatalytic behavior and anodic performance of Ti/SnO_2-Sb/Yb-PbO_2, Ti/SnO_2-Sb-PbO_2 and Ti/SnO_2-Sb-Yb anodes in sodium electrolytes were compared. The SnO_2-Sb/Yb-PbO_2 anode demonstrated better electrocatalytic performance compared with the SnO_2-Sb-PbO_2 and SnO_2-Sb-Yb electrodes in terms of both degradation and defluorination. Then a systematic experimental study was designed as follows to analyze the influencing factors: initial concentration of PFOA (10mg/L to 200 mg/L), current density (1 mA/cm^2 to 40 mA/cm^2), initial pH value (3 to 11) and electrode distance (5 mm to 20 mm). After a 150 min electrolysis, the optimum reaction conditions were obtained and the degradation and defluorination ratios reached 95.11±3.9% and 75.7±2.8%,

respectively. Under the optimum conditions, the degradation of PFOA followed pseudo-first-order kinetics (0.0193 min^{-1}) and the degradation half-life was 35.9 min. The produced F^- was measured using a fluoride ion selective electrode, whereas the intermediate PFCAs with short-chain lengths were measured using HPLC-MS. A detailed degradation pathway was proposed in this study by analyzing the intermediates and the recovery of fluoride.

Keywords: Electro-chemical degradation; Ytterbium-doped; Perfluorooctanoic acid (PFOA); Optimal conditions; Mechanisms

1. Introduction

Perfluorooctanoic acid compounds are considered important surfactants and emulsifiers because of their hydrophobic and oleophobic characteristics. Since the 1960s, the electrochemical fluorination method has been applied to the production of perfluorinated compounds, perfluorooctanoic acid, and many other kinds of perfluorinated carboxylic acids (PFCAs) and salts that contain sulfonyl perfluorinated organic compounds. Over the recent decades a large number of these products have been developed for both industrial and domestic uses [1,2]. The extensive use of these products and the strong bond energy of the C-F bond (116 kcal/mol) [3] have driven the accumulation of these compounds in various environmental niches worldwide [4-6]. In fact, these compounds have also been observed in many animal [7] and human tissues [8, 9] because of the amplification of the food chain. Some reports suggested that this class of compounds are toxic to experimental animals and humans [10, 11]. Therefore, in the fourth session of the Stockholm Conference in 2009, perfluorinated compounds including perfluorooctane sulfonic acid, perfluorooctane sulfonate and perfluorooctanesulfonyl fluoride were included in the new list of persistent organic pollutants thereby establishing the harmfulness of such substances.

Several methods for degrading perfluorinated acids under specific situations have been investigated. Among these methods, sonochemical degradation [12] and thermolysis [13] can achieve high decomposition ratios for PFOA, but these techniques require strict reaction conditions and high energy consumption. Although

the persulfate radical ($S_2O_8^{2-}$) oxidation [14] and $H_3PW_{12}O_{40}$ [15] methods can degrade PFOA under mild reaction conditions, the defluorination process is slow and inefficient. Membrane separation [16, 17], adsorption [18, 19] and ion exchange [20, 21] have also been investigated, but these merely transfer the contaminants to a second phase. The effect of disposal of the generated waste disposal on the environment and the consumption of resources must also be managed.

Unlike the above methods, electrochemical oxidation can overcome the limited oxidizing abilities of conventional advanced oxidation processes because of its many advantages, such as high oxidation efficiency, fast reaction rate, easy operation, amenable to automation, and environmental compatibility. Previous studies have demonstrated the effectiveness of boron-doped diamond, SnO_2 and PbO_2 in the degradation and mineralization of perfluorocarboxylic and perfluorosulfonic acids in a model solution [22]. Some reports have also reported the strong ability of the lead dioxide electrode in producing hydroxyl radical [23-25]. Other researchers have incorporated materials, such as Nb^{5+}[27], Bi^{4+}[28], Ce^{4+}[29], Mn^{4+}[30], and carbon aerogel [31] into the PbO_2 coating to enhance its catalytic activity for wastewater treatment [32].

In the previous report [32, 33], cerium was doped in the preparation of electrodes for degrading PFOA. Ytterbium and cesium, which both belong to Lanthanide, share the similar chemical properties. The configuration of Ytterbium is $[Xe]4f^{14}6s^2$, which is the most stable element among the rare earth (RE) element because of the saturation state. At the same time, the resistivity of Ytterbium is 28 μΩ / cm, which is the

smallest among the rare earth. The structural superiority above makes Yb^{3+} being studied extensively for many applications, such as the preparation of lithium ion batteries [34]. The the photoluminescence properties of Yb-doped Si oxide [35] have been investigated, but the performance of Yb-doped electrode in degrading PFOA by electrochemical method has been rarely examined.

In this study, we attempt to decompose PFOA using a novel Yb(III)-doped PbO_2 anode that is selected from three types of anodes (e.g., Ti/SnO_2-Sb/Yb-PbO_2, Ti/SnO_2-Sb-PbO_2 and Ti/SnO_2-Sb-Yb) and propose a decomposition pathway. We prepared and doped the electrode, investigated the effects of different factors on the electrochemical decomposition and defluorination of PFOA and studied the decomposition kinetics and defluorination pathways of PFOA by measuring the degradation rate and identifying the intermediate products. The Yb-doped anode can be an effective technology for dealing with PFOA pollution in the future.

2. Material and methods

2.1. Chemical reagents and Instruments.

$SnCl_4 \cdot 5H_2O$ (99%, Hushi, Shanghai), $SbCl_3$ (98%, Kemiou, Tianjin), HCl (36%, Tieta, Shandong), $Pb(NO_3)_2$ (99%, Damao, Tianjin), iso-propanol (99.7%, Fuyu, Tianjin), HNO_3 (68%, Kangde, Laiyang), NaF (99% , Damao, Tianjin), $Yb(NO_3)_3 \cdot 6H_2O$ (99%, Bailingwei, Beijing), Oxalic acid (99%, Xilong, Guangdong), NaOH (96%, Yongda), Na_2SO_4 (99%, Tianda, Tianjin) and Ti sheet (99%, Taiye, Baoji) were used to prepare the electrodes and for the electrolysis procedures. Perfluorooctanoic acid (PFOA, 95%) was purchased from Wongjiang (China). Perfluoropropanoic acid (PFPrA, 97%) was supplied by Aladdin (China). Perfluoroheptanoic acid (PFHpA, 98%), perfluorohexanoic acid (PFHxA, 98%), perfluoropentanoic acid (PFPeA, 97%), perfluorobutanoic acid (PFBA, 98%) and trifluoroacetic acid (TFA, 99%) were obtained from Bailingwei (China). $Na_3C_6H_5O_7 \cdot 2H_2O$ (98%, Beichen, Tianjin) and $NaNO_3$ (98%, Aibi, Shanghai) were used when measuring the concentration of fluorine ion. The instruments involoved during the experiment as follows: ultrasonic instrument (KQ-250B, Kunshanyiqi), drying cabinet (101A-2, Shuangwujin), muffle furnace (XS1-25-1200, Zhongda), pH meter (PXS-215, Lieci), magnetic stirrer (79-1, Guohua), DC power supply (DYY-6B, Liuyi). All chemicals were used without further purification and deionized water was used in all of the experiments.

2.2. Electrode fabrication.

The titanium (Ti) sheet was cut to a rectangular shape (50 mm × 20 mm, with a thickness of 0.4 mm). After polishing with two grades of sandpaper (280-grid and 600-grid), the sheets were placed in the ultrasonic instrument for 10 min to remove the particles on its surface. The sheet was then soaked in a NaOH solution (5%, m/m) at 95 ^{o}C for 1 h to remove grease. The Ti sheet was washed with distilled water and etched in boiling oxalic acid solution (10%, m/m) for about 2 h until gray pits were observed on its surface. The middle layers of the Ti/SnO_2-Sb/Yb-PbO_2 and Ti/SnO_2-Sb-PbO_2 anodes are the same, while that of the Ti/SnO_2-Sb-Yb anode is different. The coating solution was prepared as follows using the sol-gel technique: $SnCl_4 \cdot 5H_2O$ and $SbCl_3$ were dissolved in 50 ml iso-propanol at a Sn:Sb atomic ratio of 95:5. Next, 15 mL of concentrated HCl solution was added, and the resulting solution was diluted to 100 mL using iso-propanol. This solution was marked as solution A. For the Ti/SnO_2-Sb-Yb anode, we added trace ytterbium nitrate to the iso-propanol solution (which contained dissolved Sn and Sb) at a Sn: Sb: Yb atomic ratio of 95:5:0.5. This solution was marked as solution B and was used to make the Ti/SnO_2-Sb-Yb electrode only. We prepared three identical Ti sheets, of which two (marked as sheets 1 and 2, respectively) were dipped in solution A, while the other sheet (sheet 3) was dipped in solution B for 5 min. The sheets were then dried at 130°C for 10 min, and the organics were thermally decomposed at 490°C for 5 min. This dipping-annealing cycle was repeated 12 times. In the final stage, the coating was annealed for 1 h at 490^{o}C. Sheet 3 was the Ti/SnO_2-Sb-Yb electrode.

Electro-deposition was employed for the preparation of Ti/SnO_2-Sb/Yb-PbO_2 and Ti/SnO_2-Sb-PbO_2. Sheet 1 was placed into an acidic (pH 1, adjusted with HNO_3) electro-deposition solution, which contained 200 g/L $Pb(NO_3)_2$, 2 g/L NaF, and 2.36 g/L $Yb(NO_3)_3 \cdot 6H_2O$ at a constant anode current density of 20 mA/cm^2 for 90 min under room temperature (25°C). The anode was used as the Ti/SnO_2-Sb/Yb-PbO_2 electrode. Sheet 2 was treated similarly as sheet 1 except without the addition of $Yb(NO_3)_3$. The preparation of Ti/SnO_2-Sb-PbO_2 was thus completed.

2.3. Electrochemical Experiments

The 200 mL electrochemical reaction container was made of organic glass (Polymethyl Methacrylate). During the experiments, 200 ml PFOA (100 mg/L) was electrolyzed using 0.1 M Na_2SO_4 as a supporting electrolyte. The prepared Ti/SnO_2-Sb/Yb-PbO_2, Ti/SnO_2-Sb-PbO_2 and Ti/SnO_2-Sb-Yb electrodes were used as the anodes, and a same size Ti sheet was used as the cathode. The effective electrolytic area was 10 cm^2, and the stirring rate was 500 r/min. The distance between the two electrodes and the electrolysis current density can be changed. The reaction solution was sampled for analysis every 15 min or 30 min during the experiments. All experiments were performed triplicate and performed at room temperature.

2.4. Instrumental Analysis

The PFCAs concentration were measured by using a high-performance liquid chromatography-mass spectrometery (HPLC-MS, Dionex U3000, USA), which was

equipped with a Thermo C18 column (100 mm × 2.1 mm, 3 μm). A mixture of methanol (80%, volume percent) and distilled water (20%, containing 0.1% methanoic acid) was used as the mobile phase. The sample injection volume was 10 μL at a flow rate of 0.2 mL min^{-1}. Room temperature was regarded as the column temperature (25°C). Electrospray negative ionization mass spectrometry (Thermo LCQ Fleet, USA) was used to identify the intermediate products of PFOA. The capillary temperature was 320 °C. The full scan range of the mass spectra ranged from 100 m/z to 600 m/z. The gas flow rates of sheath, aux, and sweep were 30, 10 and 0 units, respectively, and the spray voltage was -4 kV. Given that the sodium sulfate electrolyte could harm the mass spectrometer, solid-phase extraction was performed to remove the salt from all samples before measurement. The analyte-specific mass spectra and standard curves of the PFCAs are shown in Figure S1 and S2(a to g) in the supporting information section.

The concentration of F^- was measured using a fluoride ion selective electrode. Given that the acidity of the electrolyzed solution (pH < 4) affects the determination of fluoride ion concentration, the total ion strength adjustment buffer (TISAB) should be added to the test solution. TISAB was prepared as follows: 58.8 g sodium citrate and 85 g sodium nitrate were dissolved in a beaker, then the pH was adjusted between 5 and 6 with HCl, and the solution was diluted to 1000 mL using distilled water. The concentration of fluoride (C_F-) and the defluorination ratio (R) were calculated as follows:

$$E = E_0 - \frac{2.303RT}{F} lg\ C_{F^-} \quad (1)$$

$$R = \frac{C_{F^-}}{C_0 \times 15} \times 100\% \quad (2)$$

where E_0 (mV) represents the steady electromotive force, E (mV) is the determined electromotive force, C_{F^-} is the concentration of fluoride ion (mg/L), and C_0 is the initial concentration of PFOA in mg/L. The stoichiometric factor of 15 indicates to the number of fluorine atoms in a PFOA molecule. Under the condition that the total ion strength in the solution is constant and sufficient, the electromotive force (E) has a linear relationship with $\lg C_{F^-}$, and $-\frac{2.303RT}{F}$ represents the slope of this line. The concentration of F^- can be obtained from the standard curve of F^- (Fig. S3).

$$ACE = \frac{(COD_0 - COD_t)FV}{8It} \times 100\% \quad (3)$$

The average current efficiency (ACE) is calculated by the formula as above. Where COD_0 and COD_t are the chemical oxygen demands (mg/L) at the initial and the final moments, respectively. The difference between COD_0 and COD_t is COD removed. F is the Faraday constant (96487C/mol), V is the volume of electrolyte (L), 8 is the equivalent mass of oxygen (g/mol), I is the current (A), and t means the electrolysis time (s).

3. Results

3.1. Selection of the anode material.

As shown in Fig. 1, under the standard reaction conditions, the degradation ratios of PFOA were 95.11±3.9%, 83.94±1.6, and 80.14±3.8% for the Ti/SnO_2-Sb/Yb-PbO_2, Ti/SnO_2-Sb-PbO_2 and Ti/SnO_2-Sb-Yb anodes, respectively. Kinetic behavior was observed and modeled as a probable pseudo-first-order reaction. The electrochemical degradation rate constants (k, k =ln Co/C) of the three anodes were 0.0193, 0.012 and 0.011 min^{-1}, respectively, and their defluorination ratios of PFOA were 76.7±2.8%, 61.4±1.1% and 52.8±2.8%, respectively, as shown in Fig. 1. According to the rate constants, the degradation h e the optimal reaction conditions. A 200 mL PFOA solution was used in the electrochemical experiments to examine the effects of current density (1 mA/cm^2 to 40 mA/cm^2), initial concentration (10 mg/L to 200 mg/L), electrode distance (5 mm to 20 mm), and initial pH (3 to 7).

3.2. Initial PFOA concentration

The effects of PFOA concentration are described in this section. Table 1 shows four samples with initial PFOA concentrations of 10, 50, 100 and 200 mg/L. The concentrations of PFOA for the three anodes were reduced by 90.90±0.1%, 93.75±0.7%, 95.11±3.9% and 83.86±2.8%, respectively (Fig. 2(a)), indicating the excellent performance of the Ti/SnO_2-Sb/Yb-PbO_2 electrode in degrading PFOA for low-concentration solutions (<100 mg/L).

Fig. 2(b), shows that with an increasing initial concentration of PFOA, the pseudo-first-order kinetic constant (k) is reduced at first, eventually increases; correspondingly, the electrochemical reaction rates increased and then decreased. This phenomenon might be explained as follows. When the concentration of initial PFOA is low (<100 mg/L), the PFOA around the anode is degraded but cannot be replenished quickly. Given the turbulence in the electrolytic cell, the PFOA located far from the anode is degraded slowly, thereby affecting the degradation rate of PFOA. In contrast, higher concentrations of shorter-chain intermediates were produced under high concentrations of PFOA. The reaction of the intermediates would consume HO· and gather on the surface of the electrode to transfer electrons, which would restrain the degradation reaction of PFOA.

3.3. Effect of current density

By influencing the electron transfer capability and the hydroxyl radical production in electrolytic systems, the current density affects the degradation and defluorination rates of PFOA [30]. Fig. 3(a) shows the different current densities (1, 5, 10, 20, 30, and 40 mA/cm^2) used to investigate the degradation of 100 mg/L PFOA. The degradation rate is very low at a low current (1 mA/cm^2), where less than 60% of the PFOA can be degraded after 150 minutes of electrolysis. Compared with this result, the degradation rate gradually increased with the increasing of applied current density. When the current density increased from 20 mA/cm^2 to 40 mA/cm^2, the rate of degradation remained above 95% and the k value increased greatly as well, to 0.0193

252 min^{-1}, 0.0234 min^{-1} and 0.0306 min^{-1} respectively.

253 As we can see from Fig.3 (b), when the X coordinate is 20 mA/cm^2, the Yb-doped
254 electrode has the highest average current efficiency (ACE). The degradation of
255 COD is low (<250 mg/L) under a low current intensity (1, 5, 10 mA/cm^2). However,
256 in spite of the high removal, a low ACE was obtained as well when the current
257 intensity is higher than 20 mA/cm^2 because of the high power consumption. This
258 experiment also proved that the 20 mA/cm^2 is the best degradation current density in
259 this electro-chemical system. This finding may be attributed to two reasons. First, the
260 mass transfer rate of PFOA molecules toward the anode is limited and the degradation
261 is inadequate. Second, the oxidation reaction at the anode is gradually enhanced by
262 the increasing applied current density. As a result, the current oversupply leads to a
263 lower average current efficiency (ACE) [36, 37].

264 **3.4. Effect of initial pH value**

265 The electrochemical degradation of PFOA was evaluated for five integral initial pH
266 values ranging from 3 to 11. Fig. 4 shows the degradation rates and the fitted
267 pseudo-zero-order kinetic curves after 150 minutes at different initial pH values.
268 When the pH value was 5, the best degradation rate of 95.11±3.9% was achieved,
269 which was 1.1 times higher than that in pH 3 and pH 7, 1.2 times higher than that in
270 pH 9, and 1.5 times higher than that in pH 11. The PFOA solutions with a lower initial
271 pH value had a higher oxidation rate than those with a higher initial pH value, thus
272 indicating that the oxidation process was more favorable in acidic solutions. This
273 conclusion also mentioned in previous literatures [38, 39]. However, low pH value
274 will increase the concentration of H^+ and hamper the positive direction to produce

275 $HO^{\cdot}$. Therefore, the trend in Fig. 4 was present. Thus, pH 5 was the most beneficial
276 pH value for the degradation of PFOA.

277 **3.5. Effect of gap distance between two plates**

278 At the same current density, the effect of different electrode gap distances on
279 degradation of PFOA is equivalent to that of electrode voltage. The degradation ratios
280 of PFOA were 95.11±3.9%, 89.05±1.1%, 85.23±1.4%, and 67.92±3.8% for the plate
281 distances of 5, 10, 15, and 20 mm, respectively (Fig. 5). As shown in Table 1, the
282 highest k value (0.0193 min^{-1}) was obtained at 5 mm, the k values of 0.0151 and
283 0.0122 min^{-1} were obtained at 10 and 15 mm, respectively; and the lowest k value
284 (0.0193 min^{-1}) was obtained at 20 mm. The $t_{1/2}$ value ranged between 35.9 min and
285 87.7 min. These data indicate that within a certain distance, a shorter electrode space
286 will lead to a higher degradation efficiency. However, the voltages between two
287 electrodes were 2.4, 2.9, 3.2 and 3.8 V for the distances of 5, 10, 15, and 20 mm,
288 respectively. The longer electrode distance, the more electrolysis time was required
289 due to the longer diffusion distance. Unlike degradation, the defluorination of PFOA
290 required higher potential to activate electron transfer. Energy-band theory argues that
291 the electron transfer reaction can be activated [33] when the energy level of an
292 unoccupied electron given by the anode is lower than that of the highest occupied
293 molecular orbital of PFOA.

294 **3.6. The production of intermediates.**

295 To investigate the production of intermediates during the electrochemical process,

HPLC-MS was used to measure the concentration of PFCAs (C_2 to C_7). As shown in Fig. 6(a), six different shorter-chain perfluoroalkyl groups (e.g., TFA, PFPA, PFBA, PFPeA, PFHxA, and PFHpA) were identified and quantified by using the mass spectra, which were produced during PFOA degradation as the intermediates. Fig. 6(a) also shows the formation of intermediates over the electrolysis time. As we can see from the diagram, during 150 min of degradation, the concentrations of PFHpA (C_7) and PFPeA (C_6) reached their maximum values at 30 min and 60 min, respectively, which decreased afterward. The concentrations of PFPeA (C_5) and PFBA (C_4) increased slightly since the beginning of electrochemical reaction but began to decrease after reaching their peaks at 90 and 120 min, respectively. The concentrations of PFPA (C_3) and TFA (C_2) slowly increased throughout the electrolysis time. The observed degradation process is similar to that seen by other researchers [30, 40]. In summary, the appearance of the maximum concentrations of the intermediates follows the order of the number of carbon atoms and PFCAs, with longer carbon chains showing higher concentrations. These phenomena indicate that the intermediates with longer chains are formed at the beginning of electrochemical reaction and are further decomposed into shorter chain intermediates as the reaction continues [33]. The incomplete degradation also indicates that some PFOA degradation products have not been fully decomposed.

$$\eta = \sum_{i=0}^{5}(3 + 2i) \times C_{CF_3(CF_2)_iCOO^-} \quad (4)$$

The mass balance of fluorine after 150 min electrolysis was investigated to analyze the electro-chemical degradation pathway of PFOA. Using Eq.(3), the mass balance

values of fluorine (i.e., { $F^-_{\text{in intermediate PFCAs, undegraded}}$ + $F^-_{\text{in PFOA, undegraded}}$ + $F^-_{\text{in solution}}$}/ $F^-_{\text{in PFOA initial}}$, $F^-_{\text{in intermediate PFCA, undegraded}}$ were calculated to be 95.8%, 95.8%, 96.8%, 95.3%, 93.6%, and 89.0% at different times, as shown in Fig 6(b). The recovery rates of fluoride were less than 100% (i.e., F^-_{unknown}), indicating that other intermediate products were quantified or detected in the solution. For example, volatile 1-C fluorocarbons may accumulate along with an increasing of electrolysis time [41]. However, the high recovery rates of fluoride allow us to describe the main reaction mechanism of the PFOA degradation in an aqueous solution.

3.7. Degradation pathway of PFOA.

Based on the results presented above and in the previous literature, a possible pathway by electrochemical oxidation could be expressed as follows: PFOA was ionized when dissolved in the solution (Eq. (5)) [42, 43]. Using the electrochemical device, PFOA underwent direct electron transfer from the carboxyl group on the anode to form perfluorooctanoic acid carboxyl radical ($C_7F_{15}COO\cdot$) (Eq. (6)). This radical was then decarboxylated to form the perfluoroheptyl radical ($C_7F_{15}\cdot$), where the method of bond cleavage was similar to the Kolbe decarboxylation mechanism in Eq. (7) [44-46].

$$C_7F_{15}COOH + H_2O \rightarrow C_7F_{15}COO^- + H_3O^+ \quad (5)$$

$$C_7F_{15}COO^- \rightarrow C_7F_{15}COO\cdot + e \quad (6)$$

$$C_7F_{15}COO\cdot \rightarrow C_7F_{15}\cdot + CO_2 \quad (7)$$

After the degradation process, $C_7F_{15}\cdot$ followed two pathways. As shown in Eq. (8), the perfluoroheptyl radical was oxidized by radical species to form $C_7F_{15}OH$ [47, 48],

which could be largely produced by the typical active electrode [23]. Given that $C_7F_{15}OH$ was a terminally unstable alcohol [49], this radical underwent intramolecular rearrangement to form $C_6F_{13}COF$ and eliminate HF (Eq. (9)) [15, 50]. The $C_6F_{13}OF$ was then hydrolyzed to form shorter-chain PFCAs by removing of CF_2 units [15] and releasing fluoride ions into the aqueous solution (Eq. (10)).

$$C_7F_{15}\cdot + HO\cdot \rightarrow C_7F_{15}OH \quad (8)$$

$$C_7F_{15}OH \rightarrow C_6F_{13}COF + H^+ + F^- \quad (9)$$

$$C_6F_{13}COF + H_2O \rightarrow C_6F_{13}COO^- + 2H^+ + F^- \quad (10)$$

In the previous literature, another reaction pathway was proposed after the Kolbe decarboxylation. In Eq. (11), the $C_7F_{15}\cdot$ reacted with the oxygen produced via water electrolysis [46]. The existence of this pathway was proven by using oxygen isotope tracers [40]. The produced $C_7F_{15}COO\cdot$ was then combined with another perfluorinated carboxylic acid radical ($RFCOO\cdot$) to form $C_7F_{15}CO\cdot$ and $RFCO\cdot$ (Eq. (12)) [29]. According to Eq. (13), the $C_7F_{15}CO\cdot$ was decomposed to produce $C_7F_{13}\cdot$ and COF_2 [46]. The obtained carbonyl fluoride was hydrolyzed to produce carbon dioxide and HF (Eq.14). In the degradation process, some volatile fluorinated organic contaminants, such as CHF_3, CF_4 and C_2F_6, may be produced during the electrolysis of the PFCs [13, 51].

$$C_7F_{15}\cdot + O_2 \rightarrow C_7F_{15}COO\cdot \quad (11)$$

$$C_7F_{15}COO\cdot + RFCOO\cdot \rightarrow C_7F_{15}CO\cdot + RFCO\cdot + O_2 \quad (12)$$

$$C_7F_{15}CO\cdot \rightarrow C_7F_{13}\cdot + COF_2 \quad (13)$$

$$COF_2 + H_2O \rightarrow CO_2 + 2HF \quad (14)$$

In the two pathways above (Eq. (5-10), and Eq. (5-7, 11-14)), PFOA was degraded to shorter-chain PFCAs by repeating the CF_2^- unzipping processes in a step-wise manner as time progressed, and PFOA was then entirely mineralized to CO_2 and F^-.

4. Conclusion

Typical anodes, such as Ti/SnO_2-Sb-PbO_2 and Ti/SnO_2-Sb-Yb, can be used in the electrochemical degradation of PFOA, whereas the addition of the rare earth ytterbium (Ti/SnO_2-Sb/Yb-PbO_2 anode) can increase the decomposition of PFOA from 83.94±1.6 and 80.14±3.8% to 95.11±3.9%. The reaction follows the pseudo-first-order kinetics, and the k values of PFOA follow the order of Ti/SnO_2-Sb/Yb-PbO_2 (0.0193 min^{-1}) > Ti/SnO_2-Sb-PbO_2 (0.012 min^{-1}) > Ti/SnO_2-Sb-Yb (0.011 min^{-1}). The degradation of PFOA showed a positive correlation with the increase of current density (1 mA/cm^2 to 40 mA/cm^2), reduction of initial concentration (10 mg/L to 200 mg/L) and shorter electrode distance (5 mm to 20 mm). The degradation rate reached to the peak at pH 5, which was higher than the other tested pH values (3 to 11). The intermediate products of PFCAs (C_2 to C_7) and fluoride ion were detected, and a possible pathway for the PFOA electrochemical degradation was proposed by analyzing the intermediate products. Compared with other metal-doped electrodes that have been recently used (between 2011 to 2015) in the decomposition of PFOA, the linear fit of the kinetic plot was k =0.0193 min^{-1}, which was higher than that of the Mn-doped electrode (0.004 min^{-1}) [30], but lower than that of the Ce-doped (0.037 min^{-1}) electrode [29]. In addition, the degradation of the Yb-doped electrode was 95.1%, which was higher than the reduction of Bi-doped electrode (93.3%) [28]. These results indicate that electro-chemical oxidation with Yb-doped electrode is an efficient method for decomposing PFOA.

Acknowledgements

The authors are grateful to the anonymous reviewers for their reading of the manuscript, and for their suggestions and critical comments.

The authors have declared no conflict of interest.

References

[1]Prevedouros, K.; Cousins, I. T.; Buck, R. C.; Korzeniowski, S. H., Sources, fate and transport of perfluorocarboxylates, Environmental science & technology, 2006, *40* (1), 32-44.

[2]Shao, T.; Zhang, P.; Jin, L.; Li, Z., Photocatalytic decomposition of perfluorooctanoic acid in pure water and sewage water by nanostructured gallium oxide, Applied Catalysis B: Environmental 2013, *142*, 654-661.

[3]Hansen, K.-J.; Johnson, H.; Eldridge, J.; Butenhoff, J.; Dick, L., Quantitative characterization of trace levels of PFOS and PFOA in the Tennessee River, Environmental science & technology 2002, *36* (8), 1681-1685.

[4]So, M.; Taniyasu, S.; Yamashita, N.; Giesy, J.; Zheng, J.; Fang, Z.; Im, S.; Lam, P. K., Perfluorinated compounds in coastal waters of Hong Kong, South China, and Korea, Environmental science & technology 2004, *38* (15), 4056-4063.

[5]Kannan, K.; Koistinen, J.; Beckmen, K.; Evans, T.; Gorzelany, J. F.; Hansen, K. J.; Jones, P. D.; Helle, E.; Nyman, M.; Giesy, J. P., Accumulation of perfluorooctane sulfonate in marine mammals, Environmental science & technology 2001, *35* (8), 1593-1598.

[6]Kannan, K.; Newsted, J.; Halbrook, R. S.; Giesy, J. P., Perfluorooctanesulfonate and related fluorinated hydrocarbons in mink and river otters from the United States, Environmental science & technology 2002, *36* (12), 2566-2571.

[7]Dai, J.; Li, M.; Jin, Y.; Saito, N.; Xu, M.; Wei, F., Perfluorooctanesulfonate and

446 perfluorooctanoate in red panda and giant panda from China, Environmental science
447 & technology 2006, *40* (18), 5647-5652.
448 [8]Conder, J. M.; Hoke, R. A.; Wolf, W. d.; Russell, M. H.; Buck, R. C., Are PFCAs
449 bioaccumulative? A critical review and comparison with regulatory criteria and
450 persistent lipophilic compounds, *E*nvironmental science & technology 2008, *42* (4),
451 995-1003.
452 [9]So, M. K.; Yamashita, N.; Taniyasu, S.; Jiang, Q.; Giesy, J. P.; Chen, K.; Lam, P.
453 K. S., Health risks in infants associated with exposure to perfluorinated compounds in
454 human breast milk from Zhoushan, China, Environmental science & technology 2006,
455 *40* (9), 2924-2929.
456 [10]Johansson, N.; Fredriksson, A.; Eriksson, P., Neonatal exposure to
457 perfluorooctane sulfonate (PFOS) and perfluorooctanoic acid (PFOA) causes
458 neurobehavioural defects in adult mice, Neurotoxicology 2008, *29* (1), 160-169.
459 [11]Johansson, N.; Eriksson, P.; Viberg, H., Neonatal exposure to PFOS and PFOA in
460 mice results in changes in proteins which are important for neuronal growth and
461 synaptogenesis in the developing brain, Toxicological sciences 2009, *108* (2),
462 412-418.
463 [12]Moriwaki, H.; Takagi, Y.; Tanaka, M.; Tsuruho, K.; Okitsu, K.; Maeda, Y.,
464 Sonochemical decomposition of perfluorooctane sulfonate and perfluorooctanoic acid,
465 Environmental science & technology 2005, *39* (9), 3388-3392.
466 [13]Krusic, P. J.; Marchione, A. A.; Roe, D. C., Gas-phase NMR studies of the
467 thermolysis of perfluorooctanoic acid, Journal of fluorine chemistry 2005, *126* (11),

1510-1516.

[14]Hori, H.; Nagaoka, Y.; Murayama, M.; Kutsuna, S., Efficient decomposition of perfluorocarboxylic acids and alternative fluorochemical surfactants in hot water, Environmental science & technology 2008, *42* (19), 7438-7443.

[15]Hori, H.; Hayakawa, E.; Einaga, H.; Kutsuna, S.; Koike, K.; Ibusuki, T.; Kiatagawa, H.; Arakawa, R., Decomposition of environmentally persistent perfluorooctanoic acid in water by photochemical approaches, Environmental science & technology 2004, *38* (22), 6118-6124.

[16]Thompson, J.; Eaglesham, G.; Reungoat, J.; Poussade, Y.; Bartkow, M.; Lawrence, M.; Mueller, J. F., Removal of PFOS, PFOA and other perfluoroalkyl acids at water reclamation plants in South East Queensland Australia, Chemosphere 2011**,** *82* (1), 9-17.

[17]Tsai, Y.-T.; Yu-Chen Lin, A.; Weng, Y.-H.; Li, K.-C., Treatment of perfluorinated chemicals by electro-microfiltration, Environmental science & technology 2010, *44* (20), 7914-7920.

[18]Yu, Q.; Zhang, R.; Deng, S.; Huang, J.; Yu, G., Sorption of perfluorooctane sulfonate and perfluorooctanoate on activated carbons and resin: kinetic and isotherm study, Water Research **2009,** *43* (4), 1150-1158.

[19]Li, X.; Chen, S.; Quan, X.; Zhang, Y., Enhanced adsorption of PFOA and PFOS on multiwalled carbon nanotubes under electrochemical assistance, Environmental science & technology 2011, *45* (19), 8498-8505.

[20]Ochoa-Herrera, V.; Sierra-Alvarez, R., Removal of perfluorinated surfactants by

490 sorption onto granular activated carbon, zeolite and sludge, Chemosphere 2008, *72*
491 (10), 1588-1593.
492 [21]Deng, S.; Yu, Q.; Huang, J.; Yu, G., Removal of perfluorooctane sulfonate from
493 wastewater by anion exchange resins: effects of resin properties and solution
494 chemistry, Water Research 2010, *44* (18), 5188-5195.
495 [22]Urtiaga, A.; Fernández-González, C.; Gómez-Lavín, S.; Ortiz, I., Kinetics of the
496 electrochemical mineralization of perfluorooctanoic acid on ultrananocrystalline
497 boron doped conductive diamond electrodes, Chemosphere 2014.
498 [23]Zhu, X.; Tong, M.; Shi, S.; Zhao, H.; Ni, J., Essential explanation of the strong
499 mineralization performance of boron-doped diamond electrodes, Environmental
500 science & technology 2008, *42* (13), 4914-4920.
501 [24]CONG YQ, Wu, ZC. Electrocatalytic Generation of Radical Intermediates over
502 Lead Dioxide Electrode Doped with Fluoride [J]. Journal of Physical Chemsitry C,
503 2007, 111(8): 3442-3446.
504 [25]HOUK LL, JOHNSON SK, FENG J, et al. Electrochemical incineration of
505 benzoquinone in aqueous media using a quaternary metal oxide electrode in the
506 absence of a soluble supporting electrolyte [J]. Journal of Applied Electrochemistry,
507 1998, 28(11): 1167-1177.
508 [26]Guohua, Z.; Xiao, C.; Meichuan, L.; Peiqiang, L.; Yonggang, Z.; Tongcheng, C.;
509 Hongxu, L.; Yanzhu, L.; Lei, L.; Dongming, Li., Electrochemical Degradation of
510 Refractory Pollutant Using a Novel Microstructured TiO_2 Nanotubes/ Sb-Doped SnO_2
511 Eletrode, Environmental science & technology 2009, *43,* 1480-1486.
512 [27] Xiupei, Y.; Ruyi, Z.; Feng, Huo.; Duochang, C.; Dan, X., Preparation and

characterization of Ti/SnO_2-Sb_2O_3-Nb_2O_5/PbO_2 thin film as electrode material for the degradation of phenol, Journal of Hazardous Materials 164(2009) 367-373.

[28]Zhuo, Q.; Deng, S.; Yang, B.; Huang, J.; Yu, G., Efficient electrochemical oxidation of perfluorooctanoate using a Ti/SnO_2-Sb-Bi anode, Environmental science & technology 2011, *45* (7), 2973-2979.

[29] Niu, J.; Lin, H.; Xu, J.; Wu, H.; Li, Y., Electrochemical mineralization of perfluorocarboxylic acids (PFCAs) by Ce-doped modified porous nanocrystalline PbO_2 film electrode, Environmental science & technology 2012, *46* (18), 10191-10198.

[30]Lin, H.; Niu, J.; Ding, S.; Zhang, L., Electrochemical degradation of perfluorooctanoic acid (PFOA) by Ti/SnO_2–Sb, Ti/SnO_2–Sb/PbO_2 and Ti/SnO 2–Sb/MnO 2 anodes, Water Research 2012, *46* (7), 2281-2289.

[31]Zhao, H.; Gao, J.; Zhao, G.; Fan, J.; Wang, Y.; Wang, Y., Fabrication of novel SnO_2-Sb/carbon aerogel electrode for ultrasonic electrochemical oxidation of perfluorooctanoate with high catalytic efficiency, Applied Catalysis B: Environmental 2013, *136*, 278-286.

[32] Niu, J.; Lin, H.; Gong, C.; Sun, X., Theoretical and experimental insights into the electrochemical mineralization mechanism of perfluorooctanoic acid, Environmental science & technology 2013, *47* (24), 14341-14349.

[33] Lin, H.; Niu, J.; Xu, J.; Huang, H.; Li, D.; Yue, Z.; Feng, C., Highly Efficient and Mild Electrochemical Mineralization of Long-Chain Perfluorocarboxylic Acids (C9–C10) by Ti/SnO_2–Sb–Ce, Ti/SnO_2–Sb/Ce–PbO_2, and Ti/BDD Electrodes,

535 Environmental science & technology 2013, *47* (22), 13039-13046.

536 [34] Qiuming Z, Yuqing Q, Minshou Z, Limin W, Structure and Eletrochemical

537 Properties of Yb-doped Lithium Iron Phosphate Cathode Materials, Journal of the

538 CHinese Society of Rare Earths, 2012, *30* (1), 78-85

539 [35] C.L. Heng, J.T. Li, W.Y. Su, Z. Han, P.G. Yin, T.G. Finstad, The formation of

540 Yb silicates and its luminescence in Yb heavily doped silicon oxides after high

541 temperature annealing, Optical Materials, 2014, *42*(1),17-23

542 [36]Thi, L.-A. P.; Do, H.-T.; Lee, Y.-C.; Lo, S.-L., Photochemical decomposition of

543 perfluorooctanoic acids in aqueous carbonate solution with UV irradiation, Chemical

544 Engineering Journal 2013, *221*, 258-263.

545 [37] Zhou, M.; Dai, Q.; Lei, L.; Ma, C. a.; Wang, D., Long life modified lead dioxide

546 anode for organic wastewater treatment: electrochemical characteristics and

547 degradation mechanism, Environmental science & technology 2005, *39* (1), 363-370.

548 [38] CONG YQ, Wu, ZC. Electrocatalytic Generation of Radical Intermediates over

549 Lead Dioxide Electrode Doped with Fluoride [J]. Journal of Physical Chemsitry C,

550 2007, 111(8): 3442-3446.

551 [39] MARTINEZ-HUITLE CA, QUIROZ MA, COMNINELLIS C, et al.

552 Electro-chemical incineration of chloranilic acid using Ti/IrO_2, Pb/PbO_2 and Si/BDD

553 electrodes. Electrochimica Acta, 2004, 50(4): 949-956.

554 [40] Zhuo, Q.; Deng, S.; Yang, B.; Huang, J.; Yu, G., Efficient electrochemical

555 oxidation of perfluorooctanoate using a Ti/SnO2-Sb-Bi anode, Environmental science

556 & technology 2011, *45* (7), 2973-2979.

[41]Zhuo, Q.; Deng, S.; Yang, B.; Huang, J.; Wang, B.; Zhang, T.; Yu, G., Degradation of perfluorinated compounds on a boron-doped diamond electrode, Electrochimica Acta 2012**,** *77*, 17-22.

[42]Chen, Y.-C.; Lo, S.-L.; Kuo, J., Effects of titanate nanotubes synthesized by a microwave hydrothermal method on photocatalytic decomposition of perfluorooctanoic acid, Water Research 2011**,** *45* (14), 4131-4140.

[43]Burns, D. C.; Ellis, D. A.; Li, H.; McMurdo, C. J.; Webster, E., Experimental p K a determination for perfluorooctanoic acid (PFOA) and the potential impact of p*Ka* concentration dependence on laboratory-measured partitioning phenomena and environmental modeling, Environmental science & technology 2008, *42* (24), 9283-9288.

[44]Dillert, R.; Bahnemann, D.; Hidaka, H., Light-induced degradation of perfluorocarboxylic acids in the presence of titanium dioxide, Chemosphere 2007, *67* (4), 785-792.

[45]Ellis, D. A.; Martin, J. W.; De Silva, A. O.; Mabury, S. A.; Hurley, M. D.; Sulbaek Andersen, M. P.; Wallington, T. J., Degradation of fluorotelomer alcohols: a likely atmospheric source of perfluorinated carboxylic acids, Environmental science & technology 2004, *38* (12), 3316-3321.

[46]Kutsuna, S.; Hori, H., Rate constants for aqueous - phase reactions of SO_4^- with C_2F_5C (O) O^- and C_3F_7C (O) O^- at 298 K, International Journal of Chemical Kinetics 2007, 39 (5), 276-288.

[47]Jing, C.; ZHANG, P.-y.; Jian, L., Photodegradation of perfluorooctanoic acid by

185 nm vacuum ultraviolet light, Journal of Environmental Sciences 2007, *19* (4), 387-390.

[48] Kormann, C.; Bahnemann, D.; Hoffmann, M. R., Photolysis of chloroform and other organic molecules in aqueous titanium dioxide suspensions, Environmental science & technology 1991, *25* (3), 494-500.

[49]Panchangam, S. C.; Lin, A. Y.-C.; Shaik, K. L.; Lin, C.-F., Decomposition of perfluorocarboxylic acids (PFCAs) by heterogeneous photocatalysis in acidic aqueous medium, Chemosphere 2009, *77* (2), 242-248.

[50]Plumlee, M. H.; McNeill, K.; Reinhard, M., Indirect photolysis of perfluorochemicals: hydroxyl radical-initiated oxidation of N-ethyl perfluorooctane sulfonamido acetate (N-EtFOSAA) and other perfluoroalkanesulfonamides, Environmental science & technology 2009, *43* (10), 3662-3668.

[51]Yamamoto, T.; Noma, Y.; Sakai, S.-i.; Shibata, Y., Photodegradation of perfluorooctane sulfonate by UV irradiation in water and alkaline 2-propanol, Environmental science & technology 2007, *41* (16), 5660-5665.

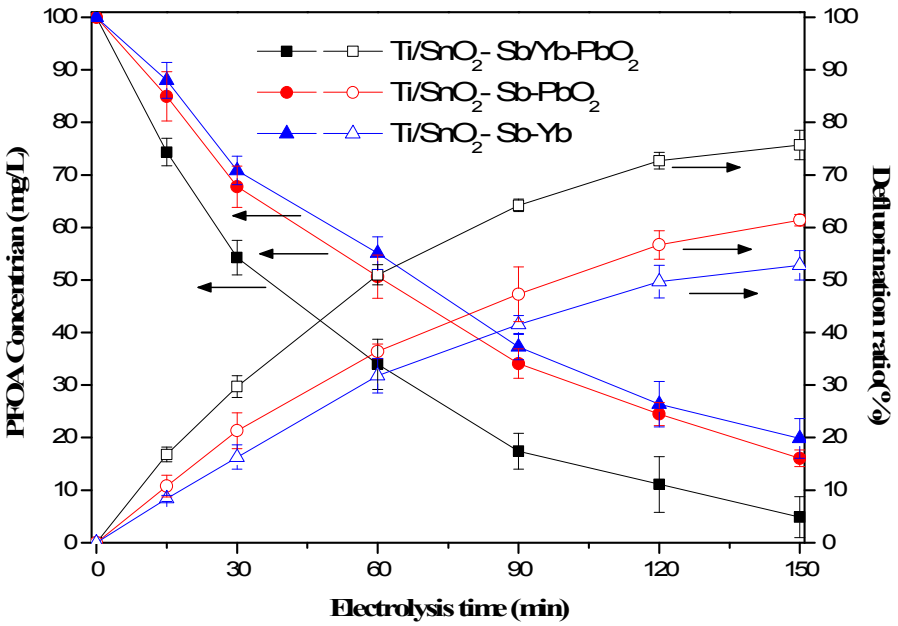

Fig. 1 Electrochemical degradation and defluorination ratio of PFOA at the reaction conditions including applied current density (20 mA/cm^2), initial concentration (100 mg/L), electrode distance (5 mm), initial pH (5) and with a 0.1 M sodium sulfate supporting electrolyte solution during 150 min, T=25 ^{o}C.

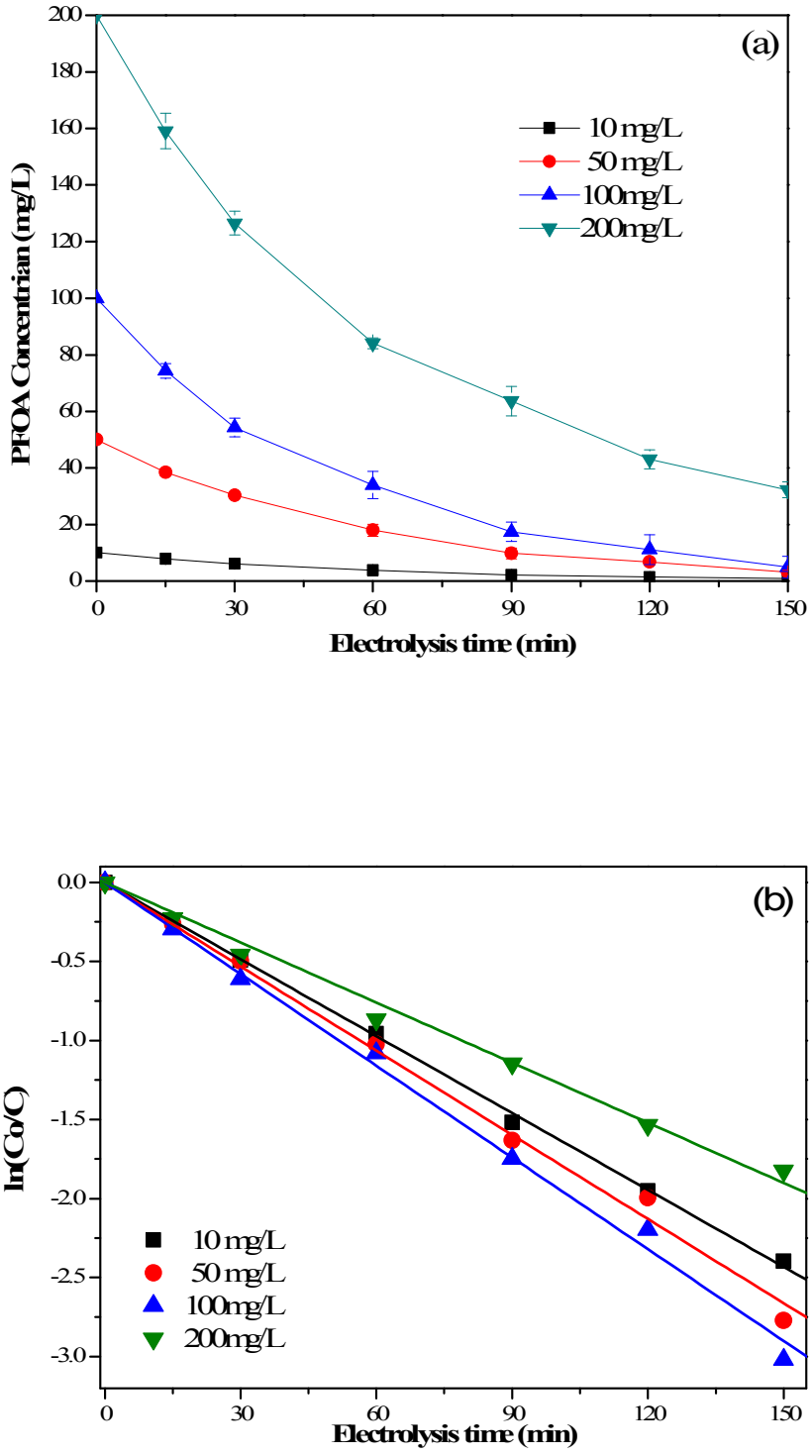

Fig. 2 (a) Effect of the initial PFOA concentration and (b) fitted pseudo-first-order kinetic curve. (Initial pH 5, plate distance 5 mm, current

density 20 mA/cm^2, 0.1 M Na_2SO_4, T=25 ^oC)

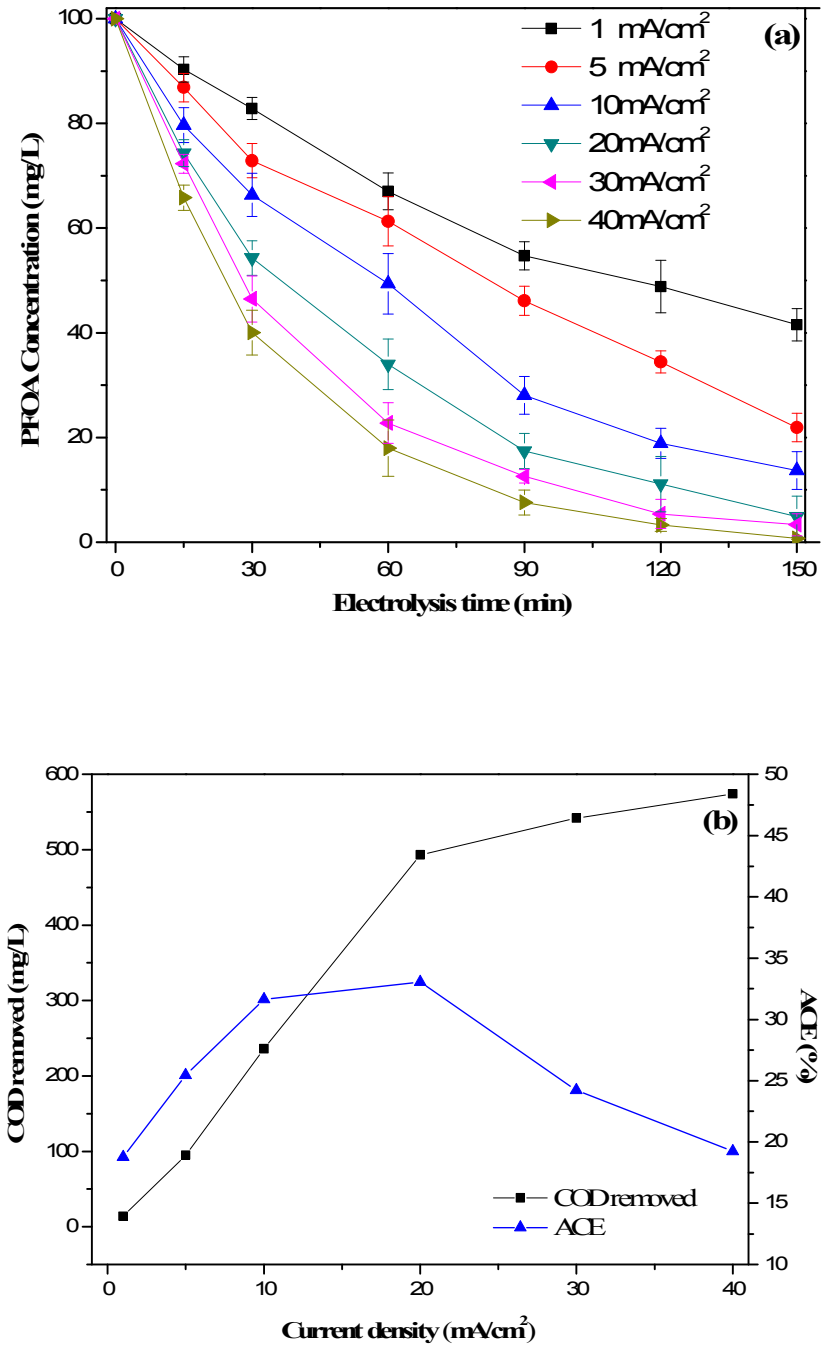

Fig. 3(a) PFOA concentration as a function of electrolysis time at current density 1, 5, 10, 20, 30, 40 mA/cm^2. Initial pH 5, plate distance 5 mm, 0.1 M Na_2SO_4,

T=25°C. (b) COD removed and average current efficiency (ACE) as a function of current density.

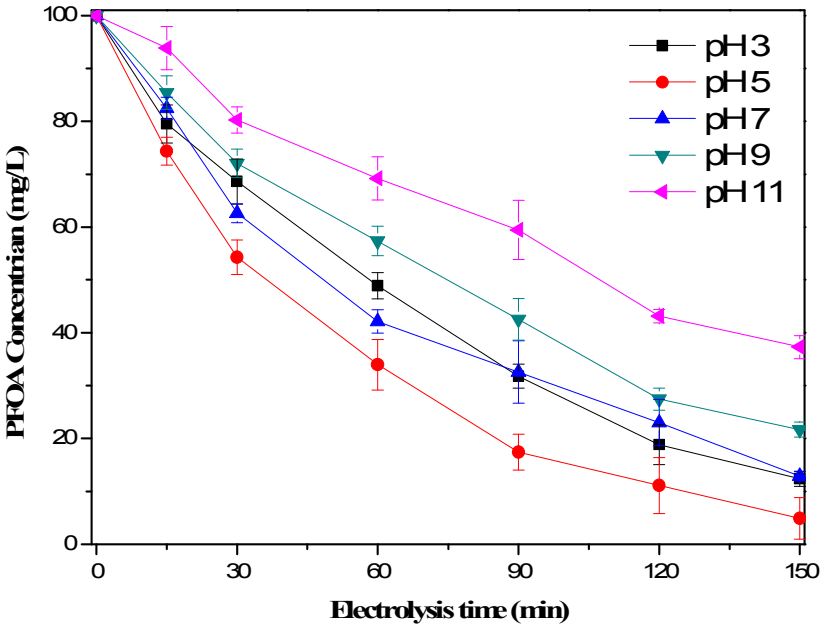

Fig. 4 Effect of initial pH value. Initial concentration 100mg/L, current density 20 mA/cm^2, plate distance 5 mm, 0.1 M Na_2SO_4, T=25 °C.

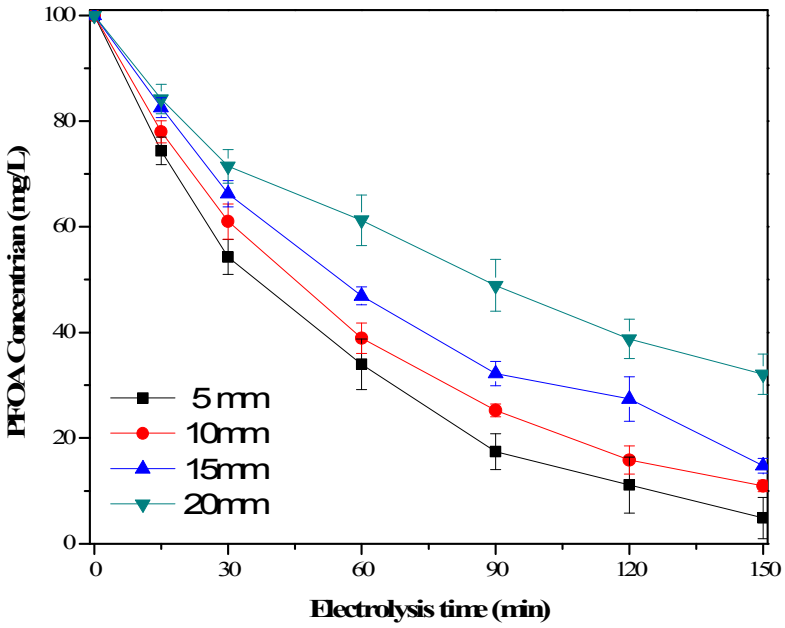

Fig. 5 PFOA concentration change as a function of electrolysis time at gap distance of 5, 10, 15, 20 mm. Initial pH 5, current density 20 mA/cm^2, initial PFOA concentration 100 mg/L, 0.1 M Na_2SO_4, T=25 ^oC.

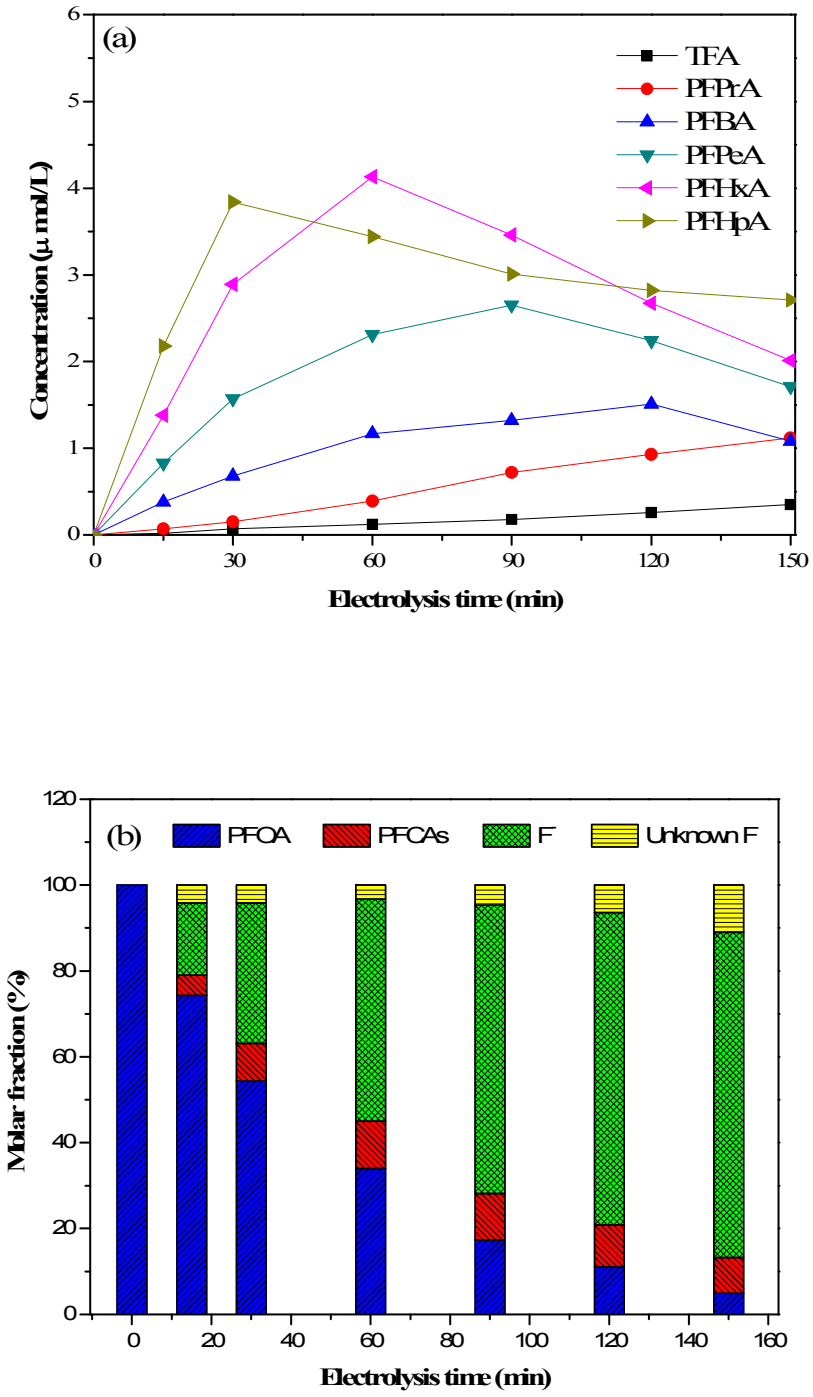

Fig. 6 (a) Concentration of intermediates (C_2-C_7) formed during electrochemical decomposition of PFOA and (b) fluorine element mass balance with the progress of reaction. The operation conditions are given in the caption of Fig. 1.

Table. 1 The efficiency and kinetics for PFOA degradation by Ti/SnO_2-Sb/Yb-PbO_2 electrode. (electrolysis time: 150 min)

Parameters		η [a]	k [b]	$t_{1/2}$ [c]	R^2 [d]
Current density (mA / cm^2)	1	58.50±3.1%	0.0061	113.63	0.991
	5	78.10±2.7%	0.0094	113.63	0.984
	10	86.33±3.6%	0.0135	51.34	0.995
	20	95.11±3.9%	0.0193	35.91	0.995
	30	96.68±2.1%	0.0234	29.62	0.997
	40	99.30±0.2%	0.0306	22.65	0.987
Initial PFOA concentration (mg/L)	10	98.10±0.1%	0.0272	25.48	0.994
	50	97.19±0.7%	0.0230	30.14	0.996
	100	95.11±3.9%	0.0193	35.91	0.995
	200	83.86±2.8%	0.0127	54.58	0.991
Initial pH value	3	87.65±1.4%	0.0139	49.87	0.994
	5	95.11±3.9%	0.0193	35.91	0.995
	7	87.13±0.9%	0.0130	53.32	0.990
	9	78.34±1.4%	0.0103	67.30	0.994
	11	62.71±2.2%	0.0067	103.45	0.988
Gap distance (mm)	5	95.11±3.9%	0.0193	35.91	0.995
	10	89.05±1.1%	0.0151	45.90	0.998
	15	85.23±1.4%	0.0122	56.82	0.986
	20	67.92±3.8%	0.0079	87.74	0.985

Other operating conditions are same as Fig. 3 - 6.

a Degradation ratio of PFOA. (%)

b Pseudo-first-order rate constant of electrochemical degradation. (min^{-1})

c The time of half-left. (min)

d Goodness of fit.